

# Calibration, Self Calibration and Astrometry

W. D. Cotton, (NRAO,SARAO), J. J. Condon (NRAO),T. Mauch (SARAO) September 4, 2020

**Abstract**—Systematic position offsets of images made with the MeerKAT array with calibrator sources distant from the target field are examined and possible causes considered. The case studied in most detail showed a nearly 2" position offset as determined from a comparison of background sources with unWISE IR positions. The effects of self-calibration were considered and found to be negligible. Limits on possible, but gross, tropospheric errors are limited to about 0.1". The expected signature of incomplete ionospheric refraction corrections was found but at a very small fraction of the total effect. Known deficiencies in the geometric calculations used in the telescope software are of the correct order of magnitude and possibly explain the observed position shift.

**Index Terms**—astrometry, calibration

## I. INTRODUCTION

**S**ELF-CALIBRATION is a powerful technique for improving the dynamic range of radio interferometer images by iteratively using the observed data with the "closure" and other constraints to improve the calibration [1]. However, one of the difficulties is that the closure constraints are invariant with shifts in the geometry and the absolute astrometric accuracy of the derived images can, in principle, be compromised. The relative locations of features in the derived image will be unaffected but the whole image may be shifted on the sky. How large this effect is depends on the details of the calculations. This memo explores the technique used in the Obit package [2]<sup>1</sup> as well as several other calibrations that affect the astrometric quality of images. This memo also presents several tests on potentially problematic data.

## II. SELF CALIBRATION AS PRACTICED IN OBIT

Most of the effects corrupting radio interferometer data are antenna based. These include the antenna electronics and the affects of the atmosphere on the astronomical signal propagating through it. In this limit, errors in calibration can be modeled with complex gains (and possibly their time and frequency derivatives) per antenna which may vary with time. The general self calibration technique as practiced in Obit consists of the following steps.

- 1) CLEAN deconvolve the data using external calibration to derive a Sky Model.
- 2) Evaluate the Fourier transform of the Sky Model (usually CLEAN components) at the locations in uv space of the measured visibilities.
- 3) Divide the Fourier transformed model visibilities into the observed visibilities. To the degree that the Sky Model

is correct, this will produce a data-set which would have been observed for a unit flux density point source with the residual calibration errors.

- 4) Solve for antenna complex gains as a function of time and frequency to derive an improved, differential, calibration.
- 5) Apply differential calibration and reimage/deconvolve.
- 6) Rinse and repeat until done.

The number of iteration of this process depends on the type of data and quality of the initial, external calibration. This can be dozens of iterations for poorly calibrated VLBI data to a few for arrays with many antennas, e.g. VLA, ALMA, MeerKAT, ASKAP. This process is not explicitly constrained to maintain astrometric accuracy.

## III. MOTIVATION FOR TEST

Recent observations with the MeerKAT array at L band involved multiple snapshots of many sources over a wide area of the sky over an 8 hour session using a single calibrator. Some of the pointings were quite far from the calibrator and the positions of background sources showed a shift of up to 2 arcseconds from IR positions of the same objects. A comparison of the apparent radio positions and the IR positions from the unWISE catalog for one field is shown in Figure 1. This shows an apparent shift of nearly 2" in the MeerKAT image. The calibrator was an ICRF source with milliarcsecond accuracy so was not the source of the position offsets. Furthermore, different targets showed different offsets, being larger for the targets more distant from the calibrator. The derived images were all the product of self calibration and the question arose, "did self cal shift the sources".

### A. Comparison of positions with and without self calibration

There is a simple test to determine if the process of self calibration introduced a position shift; compare images made with and without self calibration. One of the more discrepant fields (the field in Figure 1) was reimaged using only the external calibration from the calibrator roughly a radian away. Source catalogs were derived using Obit task FndSou. The positions of small, isolated sources brighter than 1 mJy were compared and the differences plotted in Figure 2. The flux density weighted mean RA shift was 0.003 mas and the declination shift was 0.008 mas. This is a tiny fraction of the 7.5" CLEAN restoring beam and a tiny fraction of the apparent offset of the field. The shift was not from self calibration.

The external calibration, even this far from the calibrator was not particularly bad. Self calibration only increased the flux densities of many of the brighter sources by a few percent (generally <5%), see Figure 3. In spite of the shift of nearly a quarter of the psf size, the image was not grossly distorted.

National Radio Astronomy Observatory, 520 Edgemont Rd., Charlottesville, VA, 22903 USA email: bcotton@nrao.edu

South African Radio Astronomy Observatory, 2 Fir St., Observatory, South Africa

<sup>1</sup><http://www.cv.nrao.edu/~bcotton/Obit.html>

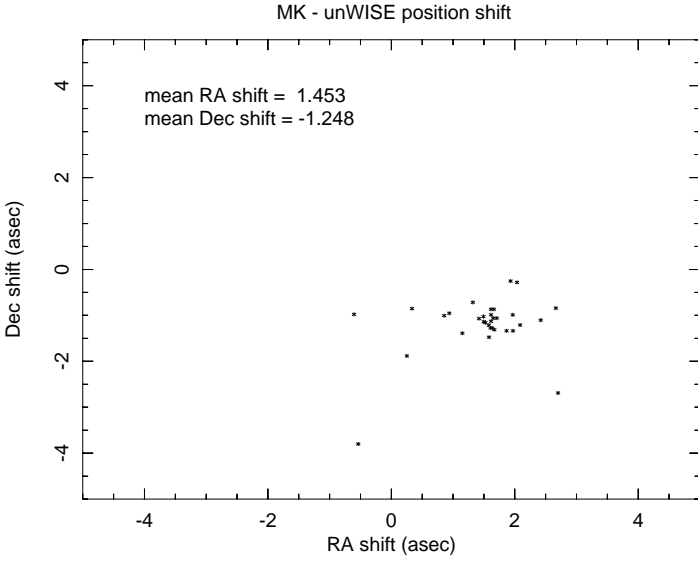


Fig. 1. Position shifts in RA and Dec between the interferometer image and the corresponding unWISE IR position. Mean shifts were radio flux density weighted.

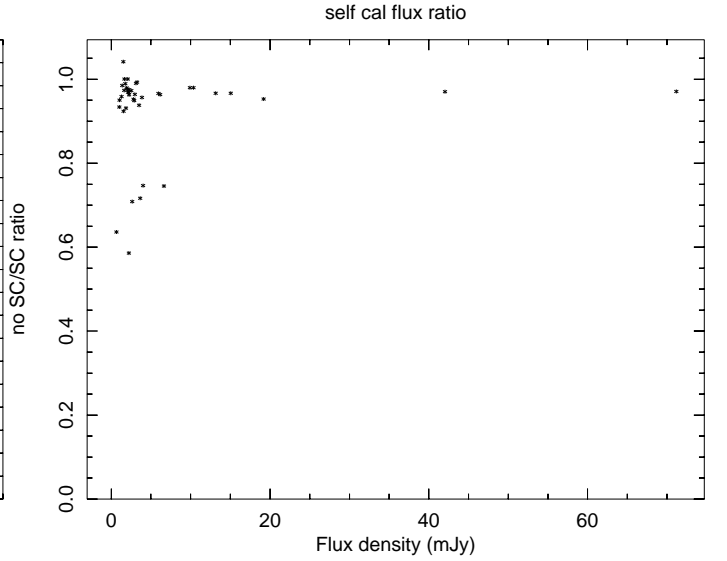


Fig. 3. Ratio of the un self calibrated peak flux densities to the self calibrated values for isolated, small sources.

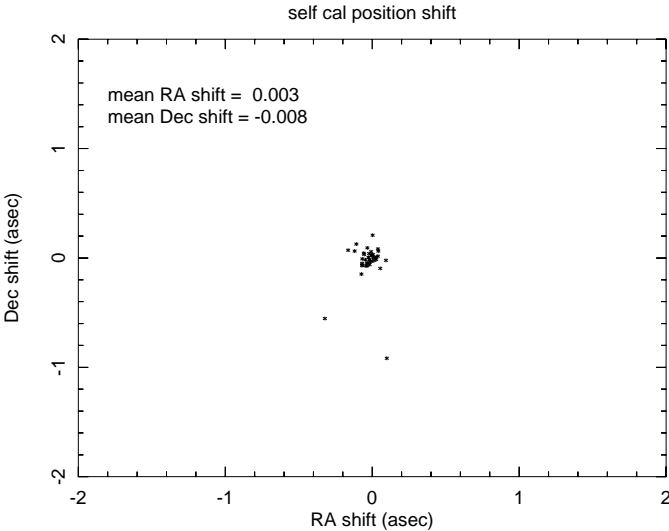


Fig. 2. Position shifts in RA and Dec between imaging with and without self calibration. Mean shifts were flux density weighted.

This suggests a systematic phase error rather than the random and time variable phase errors expected from the atmosphere.

### B. Incomplete tropospheric refraction correction

One possible source of the shift in the image coordinates is an incomplete correction for tropospheric refraction. From [3], Equation 13.20, the total zenith excess path length through the neutral atmosphere is

$$L_0 \approx 0.228P_0 + 6.3w \text{ (cm)}, \quad (1)$$

where  $P_0 \lesssim 1000$  millibars and  $w$  is the water vapor column density in cm. Thus  $L_0 \approx 2.3m$ . In the plane parallel approximation valid for baselines  $D$  much shorter than the

radius of the Earth  $r_\oplus \approx 6370$  km, the excess path length from a source at zenith angle  $z$  is  $L_0 \approx 2.3m$ . The effective thickness of the atmosphere is  $h \approx 8$  km, so the surface index of refraction is

$$n_0 \approx 1 + L/h \approx 1.0003. \quad (2)$$

Radiation entering the atmosphere at zenith angle  $z_0$  is seen at zenith angle  $z$  given by Snell's law

$$n_0 \sin(z_0) = \sin(z). \quad (3)$$

To first order (meaning, not close to the horizon), the ray is bent by

$$\Delta z \approx (n_0 - 1) \tan z, \quad (4)$$

which is  $\Delta z \approx 1'$  at  $z = 45^\circ$ . The pointing of a single dish must be corrected for this fairly large amount of refraction.

However, positions measured by a two-element interferometer depend only on the *difference* between the delays at the two antennas, so atmospheric refraction has *zero* effect in the plane-parallel approximation. The only reason that refraction matters at all is the zenith angles of two telescopes separated by  $D$  and pointing at the same source differ by of order  $D/r_\oplus$ , which is  $\sim 10^{-3}$  on a  $D \sim 6$  km baseline. The path-length change caused by this small zenith-angle difference is

$$\Delta L \sim \frac{L_0 D}{r_\oplus} \frac{\sin(z)}{\cos^2(z)} \sim 2.3 \text{ mm} \frac{\sin(z)}{\cos^2(z)} \quad (5)$$

which is only  $\sim 3$  mm at  $z = 45^\circ$  for  $D \approx 6$  km. The resulting interferometric position shift is only  $\Delta z \approx \Delta L/D \sim 0.1''$ , an order-of-magnitude smaller than the position errors in our snapshot images. Note that this angular shift is independent of baseline length, at least when  $D \ll r_\oplus$ . Unless the MeerKAT refraction correction is *badly* in error, it is not responsible for our poor snapshot astrometry.

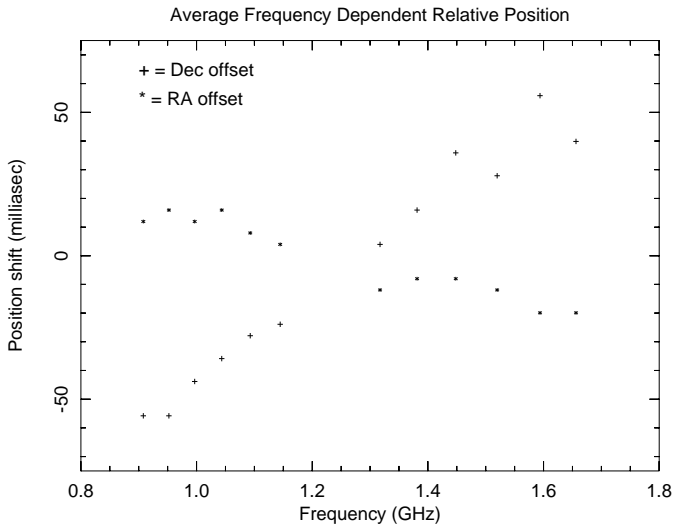


Fig. 4. Average frequency dependence of the apparent positions of three strong, small sources in the same image as Figure 1. “\*” indicate RA offset and “+” Declination offset.

#### C. Incomplete ionospheric refraction correction

Since the ionosphere is dispersive, any position shift introduced by an incomplete refraction correction will be frequency dependent, linearly proportional to wavelength. The frequency dependence of the average position relative to the wideband average for three strong, small sources in the same field as Figure 1 is shown in Figure 4. The image without self-calibration was used as self-calibration would correct such effects. Such a frequency dependent shift is seen but is far smaller than the overall position offset,  $\sim 100$  mas. The range of wavelengths in the frequency range of MeerKAT L band is 33 to 19 cm; the difference of 14 cm being nearly half of the wavelength at the low frequency end of the band. If the observed position offset were due entirely to uncorrected ionospheric refraction, the variation across the bandpass should be about half of the total observed offset. Instead it is about 1/20th of the total. Ionospheric refraction does not appear to be a major contributor to the position error.

#### D. Group Delay Errors

Errors in geometric calculations will reveal themselves in data through group delay residuals. If a correct model of the sky is available, residual delay errors can be derived from the data by the process of “fringe finding”. The apparent offset of the image represented in Figure 1 was applied to correct the coordinates of the sky model for that field and was used in Obit task Calib to determine the group delay residuals. The residuals from a selected set of MeerKAT antennas in a sequence of one minute intervals is given in Table I. The scatter of residuals in each 3 min. scan per antenna is a few picosec with relatively smooth variations in time of up to 50-60 picosec. 50 picosec corresponds to a delay error of 1.5 cm. Antenna m059 was the reference antenna (0 residual).

A memo by Ludwig Schwardt, “Correlator delay models and katpoint”, dated 29 May 2020, Figure 7, shows that the

current katpoint software used for MeerKAT differs from the more precise CALC program using earth orientation parameters (EOP) by up to 3 cm. This of the order of magnitude of the effect seen. While this is not a demonstration that the geometric approximations used are the source of the position offsets, it is very suggestive.

#### IV. DISCUSSION

The astrometric accuracy of radio interferometer images can be compromised by a large position difference between the target and the phase reference calibrator. This is a particular problem for MeerKAT due to the small antennas (large field of view) and low frequency (lots of bright sources) and the need to find a suitably bright calibrator which dominates its field; such a calibrator may be  $10^\circ$  or more away. A particularly extreme case of a MeerKAT observation where the calibrator was of order a radian from the target was examined. A comparison of background sources with unWISE positions (Figure 1) shows an astrometric error of order  $2''$  which far exceeds the nominal position accuracy. The image is shifted but not grossly distorted. Several possible causes are considered.

Self calibration has the potential for shifting positions. However, a comparison of self-calibrated and unself-calibrated images show essentially no systematic shift.

Atmospheric refraction is another suspect. Tropospheric refraction errors are considered and even a gross error would have an effect on the order of one tenth of that observed. No tropospheric refraction corrections were applied to the interferometry data. The expected frequency dependent position offset from ionospheric refraction errors was found but, again, at a level of about one tenth of the overall shift.

The approximations used in the current MeerKAT online system are known to result in delay errors of the magnitude seen in Section III-D. Deployment of planned improvements should demonstrate if this is the cause of the astrometric errors noted.

#### ACKNOWLEDGMENT

We would like to thank Ludwig Schwardt for his help understanding the MeerKAT software.

#### REFERENCES

- [1] W. D. Cotton, “A method of mapping compact structure in radio sources using vlbi observations,” *Astron. J.*, vol. 84, p. 1122, 1979.
- [2] W. D. Cotton, “Obit: A Development Environment for Astronomical Algorithms,” *PASP*, vol. 120, pp. 439–448, 2008.
- [3] A. R. Thompson, J. M. Moran, and G. W. Swenson, Jr., *Interferometry and Synthesis in Radio Astronomy, 2nd Edition*, Thompson, A. R., Moran, J. M., & Swenson, G. W., Jr., Ed. Wiley-Interscience, 2001.

TABLE I  
 SELECTED GROUP DELAY ERRORS (PICoseconds)

Time	m004	m009	m013	m018	m025	m028	m035	m040	m045	m050	m054	m059	m062
00:43:51.5	0	-0	1	9	8	6	4	-6	9	10	-4	0	-6
00:44:53.9	0	2	1	9	7	6	4	-5	13	11	-4	0	-7
00:45:48.7	-1	3	-0	7	8	7	5	-8	10	9	-7	0	-6
01:59:47.6	-1	-1	2	-5	5	-6	-1	1	6	12	-2	0	-0
02:00:46.9	-1	1	3	-1	6	-3	-2	-1	6	15	-2	0	-2
02:01:43.8	-5	-7	2	-1	4	-3	-1	-5	2	9	-3	0	-5
03:27:29.7	-1	0	-13	-5	-7	-12	2	-13	-9	5	6	0	-6
03:28:29.4	-2	4	-14	-4	-3	-13	7	-11	-8	5	7	0	-4
03:29:26.2	-7	1	-15	-4	-5	-12	11	-10	-8	6	6	0	-6
04:39:20.0	-15	-17	-23	-10	-13	-18	-4	-21	-24	-9	-2	0	-15
04:40:19.7	-13	-14	-23	-4	-8	-16	-3	-21	-20	-8	-0	0	-13
04:41:16.4	-15	-14	-23	-5	-6	-17	-3	-22	-22	-5	-1	0	-12
06:01:17.4	-30	-27	-32	-22	-22	-35	-9	-38	-40	-31	-15	0	-44
06:02:16.7	-28	-23	-32	-18	-19	-31	-4	-33	-35	-27	-13	0	-39
06:03:13.6	-29	-28	-36	-23	-22	-33	-7	-35	-36	-30	-16	0	-40
07:03:39.6	-44	-40	-43	-44	-37	-41	-31	-50	-50	-48	-29	0	-75
07:04:38.7	-39	-35	-41	-40	-34	-39	-28	-47	-45	-47	-30	0	-73
07:05:35.6	-41	-38	-45	-41	-35	-42	-28	-49	-46	-51	-33	0	-76